COMMUNICATION

Porous Antibody-Containing Protein Microparticles as Novel Carriers for ELISA

Received 00th January 20xx,

Accepted 00th January 20xx

DOI: 10.1039/x0xx00000x

Marina M. Neumann [a] and Dmitry Volodkin* [b]

The new strategy for ELISA-based detection in small volumes based on porous antibody-containing protein microparticles was developed and employed for the determination of human Immunoglobulin G demonstrating improvements in both, increase of sensitivity and reduction of antibody consumption, by ten times compared to a conventional planar ELISA.

At the present time enzyme immunoassay is one of the most widely used analytical methods in different fields of medicine, agriculture, microbiology and food industry as well as in monitoring the natural environment. This is due to the unique high affinity and specificity of the immunochemical reaction between an antigen and an antibody, and high sensitivity for the detection of an enzyme label.[1] Efficiency and miniaturization of the immunoassays for the determination of various analytes such as toxins, steroids and cancer markers are nowadays one of main challenges in portable diagnostics.

The conventional and most intensively used enzyme immunoassay is the heterogeneous enzyme-linked immunosorbent assay (ELISA). The planar geometry of the typically used support in ELISA - plastic ELISA plates - brings limitations for both the detection sensitivity and reduction of working volume of the test system. In addition, due to a limited sensitivity the consumption of expensive antibodies is rather high making the system more costly. Thus, there is a strong need to develop novel effective approaches to overcome these limitations. An obvious step to miniaturize ELISA platform and decrease the consumption of capturing antibodies or antigens is to increase the surface-to-volume ratio, for instance by using nanoparticles, optical fibers, porous hydrogel microspheres as a grafting platform or by covalent binding the capturing antibodies on ELISA plate surface instead of their hydrophobic sorption .[2]

Recently a new potent and highly sensitive enhanced chemiluminescent detection system to increase the sensitivity of ELISA via using novel substrates for the horseradish peroxidase (HRP), the traditionally used enzyme as a label in ELISA has been proposed.[3] This leads to a significant increase in the sensitivity of the analysis.

At the same time, modern approaches for encapsulation of fragile protein molecules have been developed based on porous vaterite $CaCO_3$ microcrystals.[4] The approach is based on three-step procedure: i) filling crystal pores by an appropriate method, ii) crosslinking protein-molecules physically or chemically, and iii) removal of the carbonate crystal in slightly acidic medium or by chelating agents such as ethylenediaminetetraacetic acid (EDTA) or citric acid. Mild encapsulation conditions make these sacrificial $CaCO_3$ templates very attractive to fabricate nano- and micro-particles from pure proteins with a fine control over particle dimensions, porosity, mechanical properties, and a content of a bioactive compound. The protein particles templated onto the crystals represent an inverted replica of the crystals with the pore dimensions in the range of a few tens of nanometres. Although a number of proteins have been encapsulated, to the best of our knowledge, this encapsulation approach has not been used for templating of antibody-containing particles.

Herein, the porous antibody-containing protein microparticles (PACPMs) have been synthetized via $CaCO_3$ crystal based templating and further used for ELISA analysis instead of a pure antibody (Scheme 1). The human immunoglobulin G (H.IgG) has been determined by ELISA as a model analytic compound using the goat anti-human IgG (GAH) as a specific antibody.

Scheme 1 summarizes preparation steps for PACPMs synthesis. At the first step $CaCO_3$ microcrystals containing protein mixture (GAH and BSA) were produced via co-synthesis that allows loading an enormous amount of protein into the

[a] *Fraunhofer Institute for Cell Therapy and Immunology, Am Muehlenberg 13, 14476 Potsdam, Germany*
[b] *Nottingham Trent University, Clifton Lane, Nottingham, NG11 8NS, United Kingdom*
*E-mail: dmitry.volodkin@ntu.ac.uk
Electronic Supplementary Information (ESI) available: [details of any supplementary information available should be included here]. See DOI: 10.1039/x0xx00000x

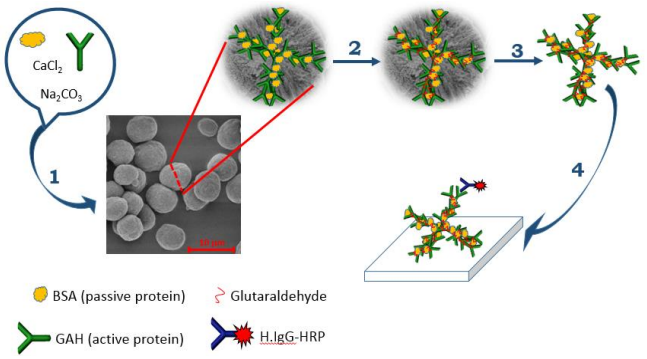

Scheme 1. Fabrication steps for PACPMs (1-3) followed by particle immobilization and immunoassay (4). 1. Co-synthesis of PACPMs using a mixture of antibodies and passive protein bovine serum albumin (BSA); 2. Crosslinking of the proteins by glutaraldehyde; 3. Template (CaCO3) removal by EDTA; 4. Immobilization of the PACPMs on the ELISA plate for the determination of H.IgG

particles with a mass content of up to tens of percent.[5] The use of passive protein BSA aims at both a reduction of costs of the expensive antibodies and an improvement of an accessibility of GAH in the particles (sterical limitations to access GAH molecules are highly likely for the pure GAH microparticles). The loading efficiency reached 70±11% (n=9). The loaded proteins were further crosslinked by glutaraldehyde followed by elimination of the $CaCO_3$ crystals by EDTA (steps 2 and 3, respectively). Finally, PACPMs have been formed and further immobilized onto a plastic surface for ELISA (step 4).

The synthesized $CaCO_3$ microcrystals and PACPMs were analyzed by scanning electron microscopy (SEM) and confocal laser scanning microscopy (CLSM). Whereas the average size of the vast majority of $CaCO_3$ microcrystals was calculated and was equal to 6 ± 2 µm, a population of microcrystals with an average diameter of 16 ± 3 µm has been revealed (3.9% of all microcrystals, n = 1505). The distribution of GAH labeled with fluorescein isothiocyanate (FITC) inside the microparticles was homogeneous before and after the removal of the carbonate cores (Fig. 1a-b). This confirms that proteins became crosslinked during the synthesis procedure and did not change their distribution after dissolving $CaCO_3$ core by EDTA. It is interesting to note that after the dissolution of the core the size of the PACPMs (Fig. 1b) decreased by 31%. This effect was also observed for other proteins, for example, insulin[6] and is related to a collapse of porous protein microparticles due to hydrophobic inter-protein interactions resulting in release of water from the microparticle pores.

SEM images in Fig. 1d-f demonstrate the formation of stable PACPMs without the presence of calcium ions (proven by EDX measurements, data not shown) that indicates a complete removal of the CaCO3 template. It is interesting to note that the average sizes of the PACPMs calculated from the SEM images were larger than those for the CaCO3 crystals used as sacrificial templates, 12 ± 3 µm for the vast majority and 25 ± 3 µm for the population with larger size, respectively. This can be explained by flattening of the PACPMs during drying procedure as required for the SEM imaging.

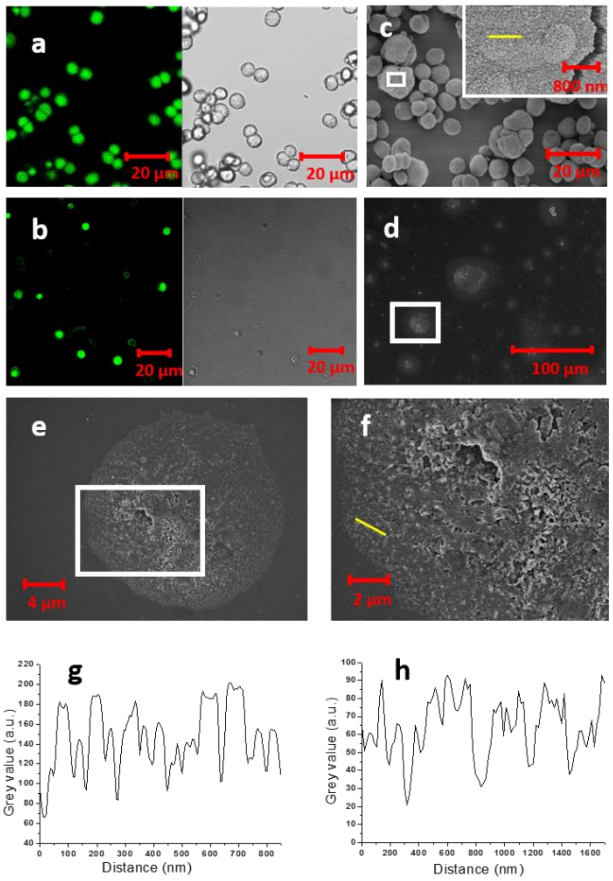

Fig. 1 CLSM (a, b) and SEM (c-f) images of PACPMs before (a, c) and after (b, d-f) template removal by EDTA. SEM image (f) represents the enlarged area in the image (e) depicted in white. Profiles (g and h) are taken along yellow lines in (c) and (f), respectively.

The porous structure of the PACPMs before and after template removal is evident from the corresponding profiles taken along to the PACPM's surface (Fig. 1 g and h). The CaCO3 crystals are made of nanocrystallines. The average sizes of the nanocrystallines and pores in PACPMs have been estimated from the width of the peaks and cavities in the profiles giving average values of 67±28 nm and 71±21 nm, respectively. As the size and shape of both PACPMs and their pores can be changed by drying during the preparation samples for the SEM analysis, we estimated sizes of nanocrystallines and PACPMs' pores by assessing the diameter of a circle of equal projection area (D_{EQPC}) [Eq. (1)]. This parameter is widely used for the evaluation of particles sizes from the projection area A of a non-spherical particle.[6]

$$D_{EQPC} = 2\sqrt{\frac{A}{\pi}} \qquad (1)$$

In this equation A is the projection area of the nanocristallines or the pores. With the help of the program Image J[7] we identified the nanocristallines/pores optically, marked them and let the program Image J calculate their projection area A. It should be noted that the study of the pore size was carried out on the edges of the dried PACPMs, where their structure is regular and well-defined.

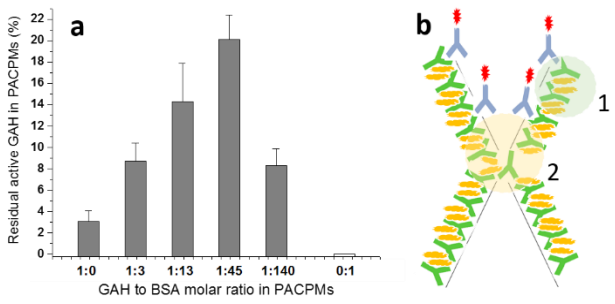

Fig. 2. The dependence of the residual active GAH in PACPMs on varying the GAH to BSA molar ratio in protein mixture (a) and the possible reasons for the low percentage of active antibodies (b). Each datum is the mean of triplicates (n=3), and the error bars represent the standard deviations of the measurements.

The porosity of the formed PACPMs greatly increases the surface area for binding antigens and thus brings significant advantages to use PACPMs in the immunoassay practice (Scheme 1, Step 4).

In the next step we have varied the ratio between GAH and BSA in the protein mixture in order to find optimal conditions for highest immunological performance of the PACPMs as indicated by the residual immunological activity of GAH in the PACPMs. Fig. 2a demonstrates that there is an optimal GAH to BSA ratio of 1:45 that provides the highest GAH residual activity of 20±2%. These PACPMs were further used in this work.

We assume that rather low residual activity and its reduction at lower and higher GAH content can be caused by sterical limitations for H.IgG to access active sites of GAH in the PACPMs. As shown in Fig. 2b, the diffusion limitations can be caused by two major problems: i) high density of GAH molecules and ii) accessibility of GAH located into small pores. The dimensions of the macromolecules used here should be taken into account for the evaluation of the diffusion limitations: GAH or H.IgG (16x12x6 nm[8]) and HRP (4x7x12 nm[9]) as a label for H.IgG.

Molecules of antigen (H.IgG or HRP-labeled H.IgG) cannot access all molecules of the specific antibodies because of rather compact packing of the GAH (Fig. 2b, 1). The reduction in the density of GAH would obviously improve the accessibility as proven by the cupola-like shape of the activity profile (Fig. 2a). On the other hand, the low residual activity can be caused by diffusion limitations for the antigen to reach the antibodies localized inside small pores (Fig. 2b, 2). This effect would be very pronounced if several molecules of HRP bind with one molecule of H.IgG during the H.IgG-HRP conjugation.

In order to prove that diffusion limitations described above can be responsible for the reduction of the GAH immunological performance, the antigen with molecular weight much lower than that of H.IgG (150 kDa) was used - fluorescent probe FITC (389 Da). The residual antibody's activity in this case rose up to 50±5% that can be caused by a better accessibility of molecules of antibodies for the smaller antigen.

Thus, the developed approach allows synthesizing stable PACPMs with active antibodies and therefore the next step

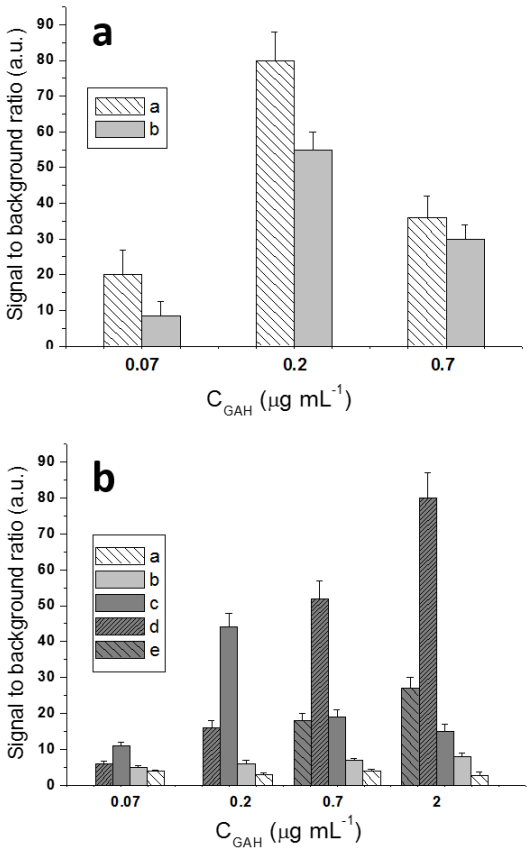

Fig. 3. The dependence of the signal to background ratio on the concentrations of H.IgG-HRP and GAH in the PACPM-based (a) and conventional (b) ELISA for the determination of the H.IgG. The dilution of H.IgG-HRP are: a – 1:10 000; b – 1:30 000; c – 1:90 000; d – 1:270 000; e – 1:810 000. Each value is the mean of triplicates (n=3), and the error bars represent the standard deviations.

was to examine immunological activity of the particles for PACPM-based ELISA and compare it with the conventional ELISA made on planar plastic surfaces. Both ELISA formats were developed in confined volume equal to 50 µL.

It is well known that different ELISA formats require specific optimal conditions for the performing of the immunoassay, mainly the certain concentrations of the used immunological reagents. Thus, firstly the optimization of each ELISA's format mentioned above was carried out (Fig. 3). The aim of the optimization was to select conditions with the use of the lowest possible concentration of the most expensive reagents, i.e. the capturing specific antibodies, and also at the same time to increase the detection sensitivity. For this, we varied concentrations of both GAH and H.IgG-HRP. The sensitivity of an assay is directly proportional to the ratio between the analytical signal and the background signal and later we relied on this ratio to assess the method sensitivity.

Fig. 3a shows the results of optimization for the PACPM-based ELISA. The results demonstrate that in the case of the lowest GAH concentration (0.07 µg mL^{-1}) the signal to background ratio is the lowest for both tested dilutions of H.IgG-HRP due to the lack of capturing antibodies and this

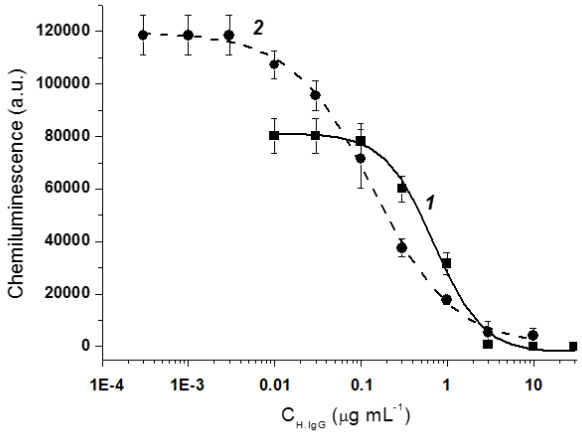

Fig. 4. Calibration curves of conventional (1) and PACPM-based (2) ELISAs. Each experimental point is the mean of four replicates (n=4), and the error bars represent the standard deviations. The favourable concentrations of reagents for the conventional and PACPM-based ELISAs are for the capturing GAH 2 and 0.2 μg mL^{-1} and for the dilution of H.IgG-HRP are 1:270 000 and 1:10 000, respectively.

leads to a low analytical signal. While using the highest concentration of GAH to 0.7 μg mL^{-1}, the background is increasing, leading by this to the lower ratio. Thus, we chose 0.2 μg mL^{-1} as an optimal concentration of GAH. Comparison of the dilution of H.IgG-HRP demonstrated that the highest ratio of analytical signal to background was received by using 1:10 000 H.IgG-HRP and was equal to 80 ± 8.

In the case of conventional ELISA the typical concentration of capturing antibodies varies between 0.2 and 15 μg mL^{-1}.[10] We focused our attention on the range of lower concentrations of the capturing GAH, which would allow us to get the signal to background ratio similar to that for the PACPM-based ELISA (Fig. 3b). For this purpose the concentration of GAH equal to 2 μg mL^{-1} was the most suitable in combination with 1:270 000 H.IgG-HRP.

At the final stage of our research we compared both variants of ELISA for the determination of H.IgG carrying out them at optimal concentrations of the capturing GAH and H.IgG-HRP (Fig. 4). The results demonstrate the typical S-shaped calibration curves for the competitive format of ELISA in both cases.

The developed new format of ELISA based on PACPMs allowed shifting the curve (2) in the area of lower concentrations of H.IgG and thus, to improve the detection limit by the factor of ten from 0.3 for conventional ELISA to 0.03 μg mL^{-1} for PACPM-based ELISA. Moreover, the benefit of using the PACPM-based ELISA was also seen in terms of the antibodies consumption, i.e. the new approach allowed decreasing the concentration of capturing antibodies also by the factor of ten from 2 to 0.2 μg mL^{-1}.

In summary, in this study the method of co-synthesis was used for the first time to fabricate PACPMs. The optimal conditions of PACPMs synthesis and the PACPMs structure have been investigated. The performance of PACPMs for practical applications as alternative to conventional ELISA has been evaluated showing significantly improved sensitivity (by an order of magnitude) and ten times reduced amount of expensive antibodies required for the analysis. We believe that this new approach could be useful in a wide range of analytical applications including medical practice and diagnostics where one seeks for a highly sensitive and cost-effective ELISA in miniaturized volumes.

The authors thank European Commission and the program Horizon 2020 for funding this project (H2020-MSCA-IF-2014_ST, 657079-IMPAM). We also thank David Šustr and Heike Runge for the help and providing of the SEM imaging. Dr. M.M. Neumann thanks Prof. I.Yu. Sakharov (Lomonosov MSU, Moscow, Russia) for the enhancer SPTZ, used in this research.

Conflicts of interest

There are no conflicts to declare.

Notes and references

1 (a) A. Johnstone and R.Thorpe, *Immunochemistry in Practice*, Wiley, Oxford, 1996, p. 384; (b) S.S.Deshpande, *Enzyme Immunoassays*, Springer, New York, 1996, p. 464.

2 (a) T. Ikeda, T. Ueda, H. Tajima, K. Sekiguchi and A. Kuroda, *Anal. Methods*., 2014, **6**, 6232; (b) F. Algaar, E. Eltzov, M. M. Vdovenko, I. Yu. Sakharov, L. Fajs, M. Weidmann, A. Mirazimi, and R. S. Marks, *Anal. Chem*. 2015, **87**, 8394; (c) A.V. Petrakova, A.E. Urusov, A.V. Zherdev and B.B.Dzantiev, *Anal. Methods*, 2015, **7**, 10177; (d) T.Liao, F. Yuan, H. Yub and Z. Li, *Anal. Methods*, 2016, **8**, 1577; (e) Z. Zhao, M. Ali Al-Ameen, K. Duan, G. Ghosh and J. F. Lo, *Biosens Bioelectron*, 2015, **74**, 305; (f) S.K. Vashist, E.M. Schneider and J.H.T. Luong, *Biosens Bioelectron*, 2015, **67**, 73.

3 (a) M.M.Vdovenko, L. Della Ciana and I.Yu. Sakharov, *Anal. Biochem.,* 2009, **392**, 54; (b) M.M.Vdovenko, A.S. Demiyanova, T.A. Chemleva and I.Yu. Sakharov, *Talanta,* 2012, **94**, 223.

4 (a) F. Tang, L. Li and D. Chen, *Adv. Mater*., 2012, **24**, 1504; (b) L. Tian, N. Gandra and S. Singamaneni, *ACS Nano,* 2013, **7**, 4252; (c) S. Schmidt, M. Behra, K. Uhlig, N. Madaboosi, L. Hartmann, C. Duschl and D. Volodkin, *Adv. Funct. Mater.*, 2013, **23**, 116; (d) W. Wei, G.-H. Ma, G. Hu, D. Yu, T. Mcleish, Z.-G. Su and Z.-Yu Shen, *J. Am. Chem. Soc.,* 2008, **130**, 15808; (e) S. Schmidt and D. Volodkin, *J. Mater. Chem. B*., 2013, **1**, 1210; (f) D.V.Volodkin, R. von Klitzing and H. Möhwald, *Angew. Chem. Int. Ed.,* 2010, **49**, 9258; (g) L. Duan, X. Yan, A. Wang, Y. Jia and J. Li, *ACS NANO,* 2012, **6**, 6897; (h) D. Volodkin, *Adv. in Col. and Interface Sci.,* 2014, **206**, 437.

5 D.V. Volodkin, S. Schmidt, P. Fernandes, N.I. Larionova, G.B. Sukhorukov, C. Duschl, H. Möhwald and R. von Klitzing, *Adv. Funct. Mater*., 2012, **22**, 1914.

6 (a) https://www.sympatec.com/en/particle-measurement/glossary/particle-shape/; (b) M. Li , D. Wilkinson and K. Patchigolla, *Particul Sci Technol*, 2005, **23**, 265.

7 Public software from National Institutes of Health; http://rsbweb.nih.gov/ij/.

8 L. J. Harris, S. B. Larson, K. W. Hasel and A. McPherson, *Biochemistry,* 1997, **36**, 1581.

9 http://www.rcsb.org/pdb/explore/explore.do?structureId=1HCH

10 (a) I.Yu.Sakharov, A.S. Demiyanova, A.V.Gribas, N.A.Uskova, E E. Efremov and M.M. Vdovenko, *Talanta,* 2013, **115**, 414; (b) J. Wang, J. Yu, Q. Yang, J. McDermott, A. Scott, M. Vukovich, R. Lagrois, Q. Gong, W. Greenleaf, M. Eisenstein, B. S. Ferguson and H. T. Soh, *Angew. Chem. Int. Ed.,* 2017, **56**, 744; (c) M.M. Vdovenko, A.S. Stepanova, S.A. Eremin, N. Van Cuong, N.A. Uskova and I.Yu Sakharov, *Food Chem.,* 2013, **141**, 865; (d) E. Sivado, S. Lareure, V. Attuil-Audenis, S. El Alaoui and V. Thomas*, Amino Acids,* 2017,**49**, 597.